Quantum Mechanical Enhancement of the Random Dopant Induced Threshold Voltage Fluctuations and Lowering in Sub 0.1 micron MOSFETs

A. Asenov, G. Slavcheva, A. R. Brown, J. H. Davies and S. Saini*

Device Modelling Group, Department of Electronics and Electrical Engineering, The University of Glasgow
Glasgow, G12 8LT, United Kingdom

* NASA Ames Research Center, Moffett Field, CA, 94035, USA

Abstract

A detailed study of the influence of quantum effects in the inversion layer on the random dopant induced threshold voltage fluctuations and lowering in sub 0.1 micron MOSFETs has been performed. This has been achieved using a full 3D implementation of the density gradient (DG) formalism incorporated in our previously published 3D 'atomistic' simulation approach. This results in a consistent, fully 3D, quantum mechanical picture which implies not only the vertical inversion layer quantisation but also the lateral confinement effects manifested by current filamentation in the 'valleys' of the random potential fluctuations. We have shown that the net result of including quantum mechanical effects, while considering statistical fluctuations, is an increase in both threshold voltage fluctuations and lowering.

Introduction

MOSFET threshold voltage variation due to statistical fluctuations in the number and position of dopant atoms becomes a serious problem when MOSFETs are scaled to sub 0.1 micron dimensions [1], [2]. This is complemented by a reduction in the average threshold voltage associated with current percolation through the random dopant induced potential fluctuations. At the same time the increase in doping concentration and the reduction in the oxide thickness in MOSFETs scaled to sub 0.1 μm dimensions results in a strong quantisation in the inversion layer, with a corresponding increase in the threshold voltage [3], and in degradation in the oxide capacitance. However, all previous 3D simulation studies of random dopant fluctuation effects [4-6] use a simple drift-diffusion approximation and do not take into account quantum effects. Until now it was unclear to what extent the quantum effects would affect the random dopant induced threshold voltage fluctuation and lowering, and to what degree the threshold voltage lowering may compensate for the increase in the threshold voltage associated with inversion layer quantisation.

In this paper we study the influence of the quantum effects in the inversion layer on the random dopant induced threshold voltage fluctuations and lowering in sub 0.1 μm MOSFETs. The quantum mechanical effects are incorporated in our previously published 3D 'atomistic' simulation approach [6] using a full 3D implementation of the density gradient (DG) formalism [7]. This results in a consistent, fully 3D, quantum mechanical picture which incorporates the vertical inversion layer quantisation, lateral confinement effects associated with the current filamentation in the 'valleys' of the potential fluctuation, and eventually tunnelling through the sharp potential barriers associated with individual dopants

Simulation approach

The DG model described in [8] was implemented in 3D in our 'atomistic' simulator but downscaled for near equilibrium (low drain voltage) conditions. This is an approximate approach for introducing quantum mechanical corrections into a macroscopic transport description by considering a more general equation of state for the electron gas, depending on the density gradient. It has been demonstrated in [8] that, to lowest order, the quantum system behaves as an ideal gradient gas for typical low-density and high-temperature semiconductor conditions. Thus a generalised drift-diffusion equation is derived including an additional term referred to as 'quantum diffusion' since its inclusion yields a theory which contains both quantum confinement effects and quantum-mechanical tunnelling. We solve self-consistently the 3D Poisson equation (1) for the potential ψ and the 3D DG approximation of Schrödinger's equation (2):

$$\nabla\cdot(\varepsilon\nabla\psi) = -q\left(p - n + N_D^+ - N_A^-\right) \tag{1}$$

$$2b_n\frac{\nabla^2\sqrt{n}}{\sqrt{n}} = \phi_n - \psi + \frac{kT}{q}\ln\frac{n}{n_i} \tag{2}$$

where $b_n = \hbar^2/(12qm_n^*)$, ϕ_n is the generalised quasi-Fermi potential, and all other symbols have the conventional meaning. The right hand side of (2) represents the Boltzmann statistics for electrons and the left hand side can be interpreted as a quantum mechanical correction to the Boltzmann statistics. At the same time (2) is a nonlinear partial differential equation, which closely resembles the Schrödinger equation, and a microscopic expression for the macroscopic factor b_n has been derived in [9]. In the iterative process the electron concentration obtained from the solution of (2) together with Boltzmann statistics for the hole concentration p are used in the solution of (1).

0-7803-5410-9/99/$10.00 © 1999 IEEE

The current at low drain voltage is extracted from the resistance of the MOSFET calculated from the electron concentration distribution by solving a simplified current continuity equation in a drift approximation only [6]. Current criterion $I_T = 10^{-8} W_{eff}/L_{eff}$ [A] is used to estimate the threshold voltage. Typically, samples of 200 microscopically different transistors are simulated for each combination of macroscopic design parameters, in order to extract the average and standard deviation of the threshold voltage.

A simulation domain used in the simulation of a 30×50 nm n-channel MOSFET with oxide thickness t_{ox} = 3 nm and a junction depth x_j = 7 nm is outlined in Fig. 1. The uniform doping concentration in the channel region $N_D = 5\times10^{18}$ cm^{-3} is resolved down to an individual dopant level using fine grain discretisation. The number of dopants in the random dopant region of each individual transistor follows a Poisson distribution. The position of dopants is chosen at random and each dopant is assigned to the nearest grid node. More complex doping profiles in the random dopant region of the device may be introduced using a rejection technique.

Standard boundary conditions are used for the Poisson equation. Dirichlet boundary conditions are applied to electrons in (2) introducing charge neutrality at the contacts and vanishing small values at the Si/SiO_2 interface. One step Newton-SOR iterations are used for solving both the Poisson (1) and the DG (2) equations. At the beginning of the iteration the nonlinear Poisson equation is solved using Boltzmann statistics for both electrons and holes.

Fig 2 illustrates the potential distribution obtained from the self consistent solution of (1) and (2) in the solution domain outlined in Fig. 1 at gate voltage equal to the threshold voltage. Strong potential fluctuations at the Si/SiO_2 interface associated with the discrete dopants can be observed. One electron equi-concentration contour which corresponds to this solution is presented in Fig. 3. The equi-concentration contour highlights the basic features of the quantum charge distribution. The quantum confinement in the channel results in a maximum in the electron concentration, located approximately 1.5 nm below the interface. We believe that the 3D solution of (2) captures the lateral confinement in current channels percolating through the 'valleys' in the fluctuation surface potential. We also believe that the penetration of the solution through sharp potential barriers associated with individual dopants represent tunnelling effects.

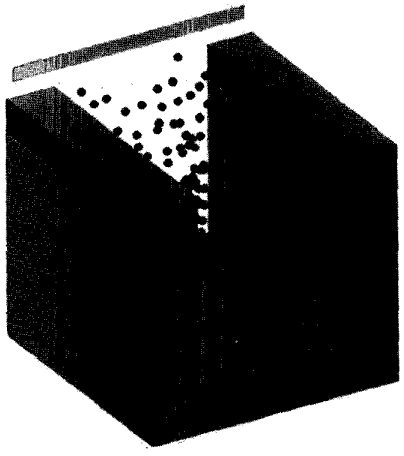

Fig. 1: Typical simulation domain and dopant distribution used in the 3D 'atomistic' DG simulation studies in this paper. It represents a 30×50 nm *MOSFET with oxide thickness* t_{ox} = 3 nm, *junction depth* x_j = 7 nm and channel acceptor concentration $N_A = 5\times10^{18}$ cm^{-3}.

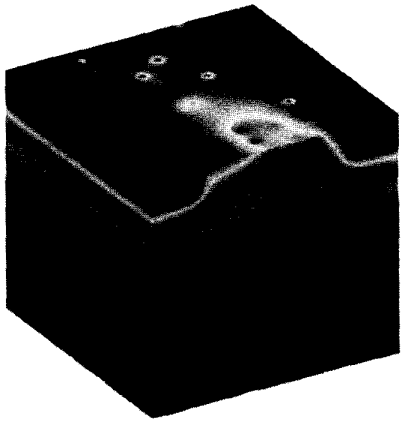

Fig. 2: Potential distribution at threshold voltage obtained from the 'atomistic' DG simulation of a 30×50 nm MOSFET with design parameters given in Fig. 1.

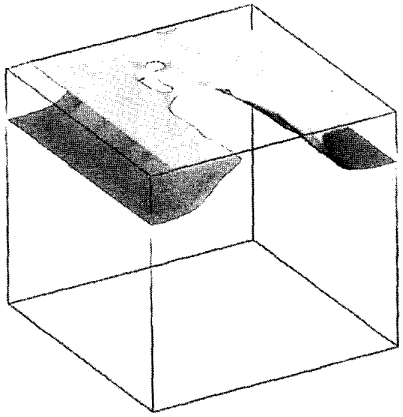

Fig. 3: One equi-concentration contour corresponding to the potential distribution in Fig. 2. The inversion charge distribution peaks below the Si/SiO_2 interface.

Calibration

Equation (2) is only an approximation to the Schrödinger equation and the DG model has to be validated against a full self-consistent solution of the Poisson-Schrödinger equation. This is a difficult task in 3D, particularly in a complex solution domain representing a MOSFET, and potential incorporating fluctuations from discrete dopants. Therefore we validate the DG approach against full band Poisson-

Schrödinger simulations [3] only in the one dimensional case and for continuous doping. Our DG results for the quantum mechanical threshold voltage shift, $V_T(QM) - V_T(Classical)$, shown in Fig. 4, using the value of electron effective mass, $m^* = 0.19m_0$, as recommended in [8], are in excellent agreement with the shift reported in [3]. The range of doping concentration used in the comparison corresponds to that of properly scaled MOSFETs with channel lengths below 100 nm. This value of m^* in the DG simulations also results in an electron concentration distribution in the inversion layer (Fig. 3) which is in close agreement with the Poisson-Schrödinger solution. Although the above value of the effective mass corresponds to the transverse electron mass in Si, there is no physical reasons for using such value in (2). Therefore we believe that the effective mass has to be treated as an adjustable parameter in the DG approach.

Fig. 5 compares the electron concentration distributions obtained using the DG model and a full band Poisson-Schrödinger simulation. The parameters in both simulations are selected to allow a direct comparison with the results presented in [3]. With an effective mass $m^* = 0.19m_0$, deduced from the comparison of the threshold voltage shifts, very good agreement between the electron distributions obtained from the two models is observed.

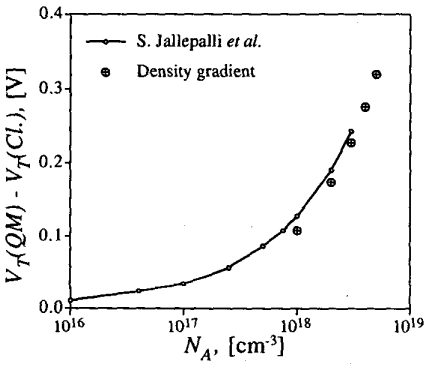

Fig. 4: Quantum mechanical threshold voltage shift as a function of the doping concentration. A comparison between DG and full band Poisson-Schrödinger results [3] for continuous doping distribution.

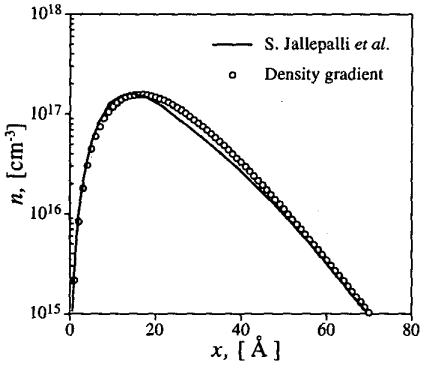

Fig. 5: Charge distribution in the inversion layer for substrate doping concentration $N_A = 5\times10^{17}$ cm^{-3}, oxide thickness $t_{ox} = 4$ nm and inversion charge density 1.67×10^{11} cm^{-2}. A comparison between DG and full band Poisson-Schrödinger results.

Results and discussion

The 'atomistically' simulated average threshold voltage $\langle V_T \rangle$ for a set of MOSFETs with different channel lengths is compared in Fig. 6 to the threshold voltage V_{T0} of devices with continuous doping. The devices have uniform doping concentration $N_D = 5\times10^{18}$ cm^{-3}, oxide thickness $t_{ox} = 3$ nm, junction depth $x_j = 7$ nm and channel width $W_{eff} = 50$ nm. Both results from classical 'atomistic' simulation and simulations including DG correction for the quantum mechanical effects are presented in the same figure.

Several interesting features associated with the inclusion of quantum mechanical effects in the 'atomistic' simulations can be deduced from Fig. 6. First of all let us consider the classical and the quantum mechanical simulations with continuous doping. The quantum mechanical shift in the threshold voltage exhibits a channel length dependence and decreases with the reduction of the channel length from 292 mV at $L_{eff} = 100$ nm to 271 mV at $L_{eff} = 30$ nm. This can be interpreted as an enhancement in the short channel effects in the quantum mechanical simulations. This is a result of an increase in effective oxide thickness associated with the location of the inversion charge centroid below the Si/SiO_2 interface.

It is well known that atomistic simulations also predict a threshold voltage lowering associated with percolation of the current through 'valleys' in the surface potential landscape. The quantum mechanical 'atomistic' simulations predict a larger threshold voltage lowering compared to the classical 'atomistic' simulations. This is illustrated in Fig. 7 where the difference between V_{T0} and $\langle V_T \rangle$ is compared for both classical and quantum mechanical 'atomistic' simulations as a function of the channel length. The threshold voltage lowering in the quantum mechanical atomistic simulations increases faster than the threshold voltage lowering in the

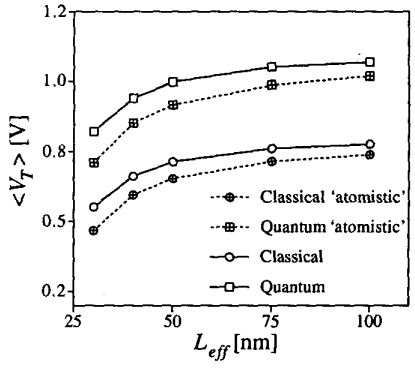

Fig. 6: Dependence of the average threshold voltage as a function of the channel length in MOSFETs with $W_{eff} = 50$ nm, $N_A = 5\times10^{18}$ cm^{-3} and $t_{ox} = 3$ nm. The quantum mechanical shift in the threshold voltage decreases as the channel length is reduced.

classical simulations with the reduction of the channel length. This can be interpreted again as an additional enhancement of the short channel effects in the quantum mechanical case. The threshold voltage lowering, which reaches more than 110 mV in a 30 nm MOSFET, compensates for a significant portion of the quantum mechanical threshold voltage shift.

Finally, Fig. 8 compares channel length dependence of the standard deviations in the threshold voltage σV_T calculated using classical and quantum mechanical 'atomistic' simulations. The quantum mechanical simulations predict an increase in σV_T compared to the classical case which is more pronounced at the shorter channel lengths and ranges from 23.4% at the 100 nm MOSFETs to 24.6% at transistors with 30 nm channel length. The possible explanation of this effect is the reduction in the effectiveness of the screening of the random potential fluctuations by the inversion layer charge displaced from the interface as a consequence of the quantisation perpendicular to the interface. Additional simulation experiments and theoretical investigations are required in order to understand better the mechanism responsible for enhancement of the threshold voltage fluctuations in the quantum mechanical atomistic simulations.

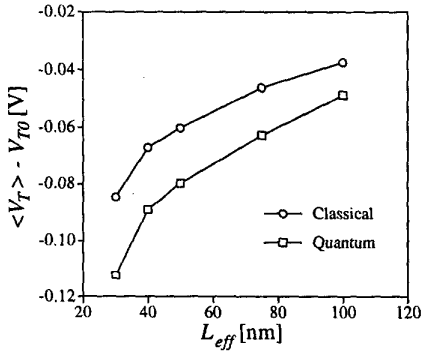

Fig. 7: Threshold voltage lowering as a function of the channel length extracted from the data in Fig. 6. A comparison between classical and quantum mechanical atomistic simulations.

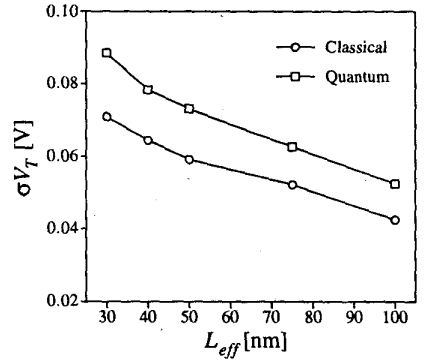

Fig. 8: Dependence of the threshold voltage standard deviation as a function of the channel length for the devices from Fig. 6.

Conclusions

In this paper we demonstrated that accounting for the quantum effects in 'atomistic' simulations results in an increase in both threshold voltage fluctuations and lowering. The quantum enhancement in the threshold voltage uncertainty amounts to more than 50% in MOSFETs with oxide thicknesses below 1.5 nm, expected near the end of the Roadmap. The raising of the threshold voltage when quantum effects are taken into account is partially compensated by the threshold voltage lowering due to 'atomistic' effects. This compensation varies from 16% in 100 nm MOSFETs up to 40% in 30 nm devices.

Acknowledgment

This work is supported by NASA Ames Research Centre grant NAG 2-1241.

References

[1] T. Mizuno, J. Okamura and A. Toriumi, "Experimental study of threshold voltage fluctuation due to statistical variation of channel dopant number in MOSFET's", *IEEE Trans. Electron Devices*, vol. 41, pp. 2216-2221, 1994.

[2] J. T. Horstmann, U. Hilleringmann, and K.F. Gosser, "Matching analysis of deposition defined 50-nm MOSFET's", *IEEE Trans. Electron Devices*, vol. 45, pp. 299-306, 1997.

[3] S. Jallepalli, J. Bude, W.-K. Shih, M. R. Pinto, C. M. Maziar and A. F. Tasch, Jr., "Electron and hole quantisation and their impact on deep submicron silicon p- and n-MOSFET characteristics", *IEEE Trans. Electron Devices*, vol. 44, pp. 297-303, 1997.

[4] Wong H.-S. and Taur Y. "Three dimensional 'atomistic' simulation of discrete random dopant distribution effects in sub-0.1 μm MOSFETs", *Proc. IEDM'93. Dig. Tech. Papers.*, pp. 705-708.

[5] P. A. Stolk, F. P. Widdershoven, and D.B.M. Klaassen, "Modeling statistical dopant fluctuations in MOS Transistors", *IEEE Trans. Electron Devices*, vol. 45, pp. 1960-1971, 1998.

[6] A. Asenov, "Random Dopant Induced Threshold Voltage Lowering and Fluctuations in Sub 0.1 μm MOSFETs: A 3D 'Atomistic' Simulation Study", *IEEE Trans. Electron Devices*, vol. 45, pp. 2505-2513, 1998.

[7] M. G. Ancona and H. F. Tiersten, "Microscopic physics of the Silicon inversion layer", *Physical Review B*, vol.35, pp. 7959-7965, 1987.

[8] C.S Rafferty, B. Biegel, Z. Yu, M.G. Ancona, J. Bude and R.W. Dutton, "Multi-dimensional quantum effects simulation using a density-gradient model and script-level programming technique", *SISPAD'98*, Eds. K. De Meyer and S. Biesemans, pp. 137-140, 1998.

[9] M. G. Ancona and G. I. Iafrate, "Quantum correction to the equation of state of an electron gas in a semiconductor", *Physical Review B*, vol.39, pp. 9536-9540, 1989.